Geomorphology 180–181 (2013) 267–280

Contents lists available at SciVerse ScienceDirect

Geomorphology

journal homepage: www.elsevier.com/locate/geomorph

Basin-scale and travertine dam-scale controls on fluvial travertine, Jiuzhaigou, southwestern China

J.L. Florsheim [a,*], S.L. Ustin [a], Y. Tang [b], B. Di [b], C. Huang [b], X. Qiao [b], H. Peng [b], M. Zhang [a], Y. Cai [c]

[a] University of California, One Shields Ave., Davis, CA, 95616, USA
[b] Department of Environment, Sichuan University, Moziqiao, Chengdu, Sichuan, 610065, China
[c] Jiuzhaigou Administrative Bureau, Jiuzhaigou County Aba Municipality, Sichuan, 623400, China

ARTICLE INFO

Article history:
Received 15 May 2012
Received in revised form 10 October 2012
Accepted 16 October 2012
Available online 23 October 2012

Keywords:
Travertine
Tufa
Fluvial
Morphology
Jiuzhaigou
China

ABSTRACT

Travertine deposition in fluvial systems builds dams and other forms that create diversity in geomorphic processes, morphology, and associated wetland ecosystems. In Jiuzhaigou Natural Reserve, Sichuan Province, China, we investigate the relation between contemporary fluvial travertine morphology, slope, and water chemistry at the fluvial-system scale and at the local scale of large individual dams in order to address two fundamental questions. First, what factors determine the spatial distribution of such large valley-spanning, or *primary*, travertine dams? Second, what factors govern smaller but distinctive travertine dams and other *secondary* travertine morphology present on the sloping downstream side of primary travertine dams? Through remote sensing analysis and field work, we recognize two factors as paramount in controlling spatial distribution of primary fluvial travertine dams: watershed-scale steps in the longitudinal profile and water chemistry, based on a proxy for dissolved calcite. In the steep Jiuzhaigou watershed, hillslope erosion processes that contribute large boulders to the channel influence the majority of the primary dams. However, two valley-spanning primary dams, Pearl Shoals and Norilang Lakes, appear to be dominated by travertine precipitation. The submerged upstream sides of these two dams are nearly vertical with heights > 30 m. Slope varies with position along the longitudinal profiles over the downstream sides of these two primary dams because the profile shapes are convex. With downstream-dam profile lengths > 500 m, flow encounters secondary travertine morphology organized as an array of travertine bedforms that vary with local channel slope along the convex profiles. The secondary travertine bedforms include sequences of repeating patterns including smaller dams that impound correspondingly small waterbodies. Morphologic differences between two types of secondary dams are quantified on the basis of their relative size, spacing, and the slope on which they form. Increasing slope is correlated with a decrease in height of secondary travertine bedforms according to a power law where $y = 0.0053x^{-1.68}$. Results of the investigation demonstrate that slope, a main influence on river hydrodynamics, influences and is influenced by fluvial travertine morphology at two discrete fluvial scales. This work advances our understanding of geomorphic factors that influence travertine morphology, a critical need for conservation and management of travertine natural resources and their wetland ecosystems.

1. Introduction

Travertine, a sedimentary rock formed by chemical precipitation of calcium carbonate, is an integral component of ambient temperature fluvial systems in carbonate landscapes. An example is Jiuzhaigou National Nature Reserve, Sichuan Province, China (Fig. 1), listed by the UNESCO as a World Natural Heritage Site and a Man and Biosphere Reserve because of its superlative landscape that includes stream segments separated by waterfalls. Some of the waterfalls are formed by travertine dams that impound clear lakes exhibiting a dramatic range of blue-green colors. Understanding geomorphic processes that influence travertine development is important in the conservation of this natural and cultural resource and the significant wetland ecosystems formed on travertine substrate. Fluvial travertine in ambient temperature fluvial systems is often called tufa and sometimes sinter (Ford and Pedley, 1996; Pentecost, 2010). However the terms tufa and travertine are often used interchangeably in the literature (Pentecost and Viles, 1994), and here we follow the terminology used by Pentecost (2005, 2010) and use the term travertine to characterize the precipitated carbonate landforms that exemplify the morphology at Jiuzhaigou.

Travertine precipitates from water supersaturated with respect to calcium carbonate (Andrews et al., 1993) through physical, chemical, and biological mechanisms (Liu et al., 1995; Viles and Pentecost, 1999; Wright, 2000; Chen et al., 2004; Pentecost, 2005; Goldenfeld et al., 2006; Pedley and Rogerson, 2010). Travertine precipitation follows the reaction:

$$Ca^{2+} + 2HCO_3^- \leftrightarrow CaCO_3 + CO_2 + H_2O$$

* Corresponding author.
E-mail addresses: jl.flors@gmail.com, florsheim@ucdavis.edu. (J.L. Florsheim).

0169-555X/$ – see front matter © 2012 Elsevier B.V. All rights reserved.
http://dx.doi.org/10.1016/j.geomorph.2012.10.016

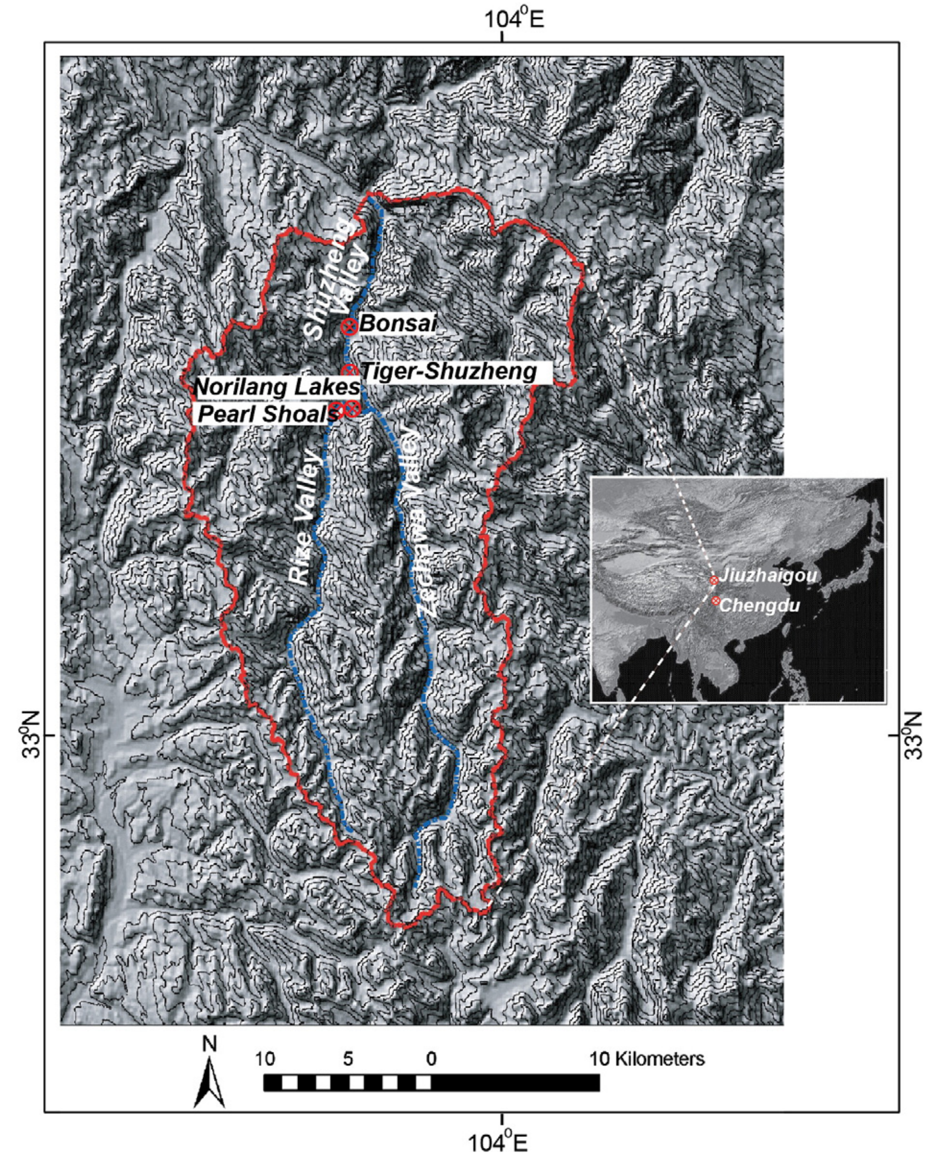

Fig. 1. Location of watershed encompassing Jiuzhaigou National Nature Reserve, Sichuan Province, China, showing Rize, Shuzheng, and Zechawa valleys. Symbols indicate location of field sites where longitudinal profiles were measured at Pearl Shoals, Norilang Lakes, Tiger, Shuzheng, and Bonsai travertine dams. Elevation at the basin mouth is 2000 m and the highest elevation greater than 4550 m.

where the terms on the left-hand side of the reaction represent calcium (Ca^{2+}) and bicarbonate ($2HCO_3^-$) ions dissolved in the water. On the right-hand side of the reaction, calcium carbonate ($CaCO_3$), or travertine precipitation, is driven by degassing of carbon dioxide (CO_2) to the atmosphere. Previous work largely represents studies conducted at hot springs, whereas limited data are available for ambient temperature fluvial travertine systems, e.g. travertine rivers.

Both biological and physical factors influence travertine formation. Biological factors influence the process by modifying CO_2 concentrations through the uptake of CO_2 gas during photosynthesis (Herman and Lorah, 1987; Viles and Goudie, 1990) and the release of CO_2 during respiration. Microbes may accelerate travertine precipitation through metabolic processes that either increase alkalinity that lowers travertine solubility or that produce substances providing nucleation sites for mineral precipitation (Riding, 2000)—both of which are processes that occur in ambient temperature and hot spring systems (Foulke, 2011). Organisms such as bacteria, algae, and fungi contribute to the growth of microbial biofilms and mats that alter CO_2 concentrations through photosynthesis and respiration. In addition, plant surfaces provide substrates for crystal nucleation (Golubic, 1973; Wright, 2000) and algae and bryophytes (mosses) can be integral to travertine precipitation. Pentecost and Zhang (2000) observed that a combination of abiotic and biotic factors contributes to travertine precipitation at Jiuzhaigou.

In ambient temperature rivers, numerous hydrodynamic factors promote travertine precipitation along with biological factors. Significantly, flume studies report that turbulent flow caused by the presence of waterfalls or other topographic irregularities aerates flow, causes bubbles, and forms spray that increases the air–water interface area, lowers the fluid pressure and thus enhances CO_2 degassing (Chen et al., 2004). Further, lower fluid pressure resulting from flow acceleration may occur along topographic irregularities and obstacles in the channel boundary. The water pressure in such zones decreases as described by the Bernoulli effect, and dissolved CO_2 gas may preferentially be released in such locations (Chen et al., 2004).

Previous work recognized that geomorphology influences travertine landform development (Pentecost and Viles, 1994; Merz-Preiss and

Riding, 1999) and has explored physical and environmental controls on travertine deposition in fluvial systems globally (Ford and Pedley, 1992). However, limited data quantify the dominant geomorphic parameters that strongly influence formation, evolution, or diversity of travertine forms at the watershed system scale and at local travertine landform scales. Nonetheless, the role of geomorphic and chemical parameters on the spatial distribution of travertine dams and the effect of geomorphic parameters such as slope on morphologic diversity of travertine bedforms are critical to understanding travertine geomorphology in fluvial systems. This paper reports results of a remote sensing and field investigation in Jiuzhaigou to investigate two fundamental questions regarding travertine geomorphology: (i) what factors determine the spatial distribution of large travertine dams and (ii) what factors control variations of travertine morphology at the scale of the basin vs. the scale of an individual travertine landform?

We used high resolution satellite imagery and currently available topographic data to document spatial variation in basin-scale channel gradient and channel width, and we sampled water quality throughout the basin to address the first question. We conducted field measurements of slope, bedform height, and spacing at five large valley-spanning travertine dams to quantify factors that control variation of organized sequences of smaller travertine bedforms that characterize travertine morphology. In particular, we explored the influence of local channel gradient on the morphology of a distinct sequence of travertine bedforms formed atop larger travertine dams that form watershed-scale steps in the longitudinal profile.

Our results suggest that geomorphic parameters influence and are influenced by fluvial travertine morphology at two discrete fluvial scales. This work adds to our fundamental knowledge of fluvial travertine system formation and has relevance toward management of these sensitive landforms at Jiuzhaigou and in other fluvial travertine systems globally.

Our results advance our understanding of the geomorphic processes that influence the development of fluvial travertine morphology and patterns in a complex fluvial field setting and may be used to validate future laboratory or modeling predictions that explore the influence of slope on morphology, height, and spacing of fluvial travertine bedforms.

2. Travertine morphology

2.1. Travertine dams

Precipitation of travertine on smooth surfaces or as bedforms results from interactions between physical (Herman and Lorah, 1988; Liu and Dreybrodt, 1997; Chen et al., 2004) and biotic factors (Pentecost and Zhang, 2001; Pentecost, 2010; Fuller et al., 2011). Aside from structures associated with travertine precipitation at scales on the order of centimeters or smaller that result from interactions of supersaturated water with mosses and microbes such as algae, the most common travertine morphologies described in fluvial systems are dams (Pentecost and Viles, 1994; Liu et al., 1995; Ford and Pedley, 1996; Lu et al., 2000; Pena et al., 2000; Pentecost and Zhang, 2000; Wright, 2000; Zhang et al., 2001; Pedley et al., 2003; Moeyersons et al., 2005; Pentecost, 2005; Andrews, 2006; Carthew et al., 2006; Dreybrodt and Gabrovsek, 2009; Pentecost, 2010; Fuller et al., 2011). Small travertine dams are also recognized as a characteristic landform in thermal travertine systems (Veysey and Goldenfeld, 2008; Foulke, 2011).

Actively forming travertine dams have been identified in fluvial systems globally (Ford and Pedley, 1992, 1996). Pentecost (2005, 2010) describes fluvial travertine dams as perpendicular to the direction of local flow with somewhat sinuous crests, whereas other researchers note that some dams have convex downstream arcuate planforms (Carthew et al., 2006). Travertine dams impound water in upstream lakes (Ford and Pedley, 1992; Pedley et al., 2003). Deep water slowly flows from each lake until it reaches the crest of the dam where flow depth shallows and velocity accelerates with steeper slope and high velocity flow along the downstream side of the dam.

2.2. Repeating travertine patterns: aka fluvial travertine bedforms

Previous studies recognize that spatial heterogeneity of travertine precipitation creates bedforms with repeating patterns, analogous to the way that alluvial rivers are characterized by organized bedform sequences. For example, when calcite precipitates from water flowing over a surface, multiple ridges form perpendicular to the flow direction, and pools form upstream of the ridges—forming a characteristic pattern that ranges in size from centimeters to hundreds of meters (Hammer, 2009). Travertine bedforms classified as dams or steps in ambient temperature fluvial systems are analogous to such ridges, whereas analogous bedforms described in thermal travertine systems include small dams separated by terraces—relatively level areas where water may be ponded upstream of the small dam. Such morphology, referred to as 'terrace and rimstone' dams in thermal systems has also received recent attention. Recent numerical modeling of these iconic travertine patterns has investigated factors influencing their formation including slope (Jettestuen et al., 2006) and flow rate (Hammer et al., 2007; Veysey and Goldenfeld, 2008). In addition, field studies identified the influence of microbial activity (Foulke, 2011) on their development.

Previous work in Jiuzhaigou and other similar travertine systems documented the presence of repeating travertine bedforms by documenting the spacing of relatively large travertine dams (Pentecost and Zhang, 2001; Pentecost, 2005, 2010). Pentecost (2010) referred to large dams as 'macrodams' with a spacing of 4 km at Jiuzhaigou and, based on this work and work from other travertine systems, suggested a general rule: dam spacing decreases on steeper slopes (Pentecost, 2010). Other researchers (Hammer et al., 2007; Veysey and Goldenfeld, 2008) suggest that spacing of multiple travertine dams may be influenced by competition, whereby a fast-growing downstream dam may flood a slower growing upstream dam, hindering its growth and accordingly lengthening the characteristic wavelength between actively growing or dominant dam crests.

2.3. Influence of positive feedback on growth of travertine morphology

Repeating sequences of dams and intervening pools or terraces affect river hydrodynamics and, with positive feedback, promote their own growth (Goldenfeld et al., 2006; Jettestuen et al., 2006; Chan and Goldenfeld, 2007; Hammer et al., 2007). The flume studies conducted by Chen et al. (2004) suggest that this occurs because hydrodynamic diversity promotes carbon dioxide degassing and drives travertine precipitation. The numerous physical conditions and mechanisms leading to the localized positive feedback of travertine precipitation on dams in natural travertine systems summarized by Hammer (2009) include shallower water depth, increased turbulence, higher flow velocity, and increased mixing across the ridge—and these conditions interact to decrease fluid pressure and increase degassing of carbon dioxide that promotes travertine deposition at rates higher than either mechanical erosion or chemical dissolution. The positive feedback occurs because the new travertine deposition enhances the physical conditions and mechanisms that promote carbon dioxide degassing and travertine deposition. Chan and Goldenfeld (2007) suggest that travertine forms are scale-invariant and that travertine precipitation rates are characterized by non-linearity because the travertine surface changes as travertine precipitates. Moreover, biofilms or other organic material may adhere to the obstruction created by a travertine dam, further enhancing its growth.

Besides indicating the relevance of physical factors such as slope and flow velocity in travertine pattern formation (Jettestuen et al., 2006; Hammer et al., 2007; Veysey and Goldenfeld, 2008), simulations conducted by Hammer et al. (2007) and Veysey and Goldenfeld (2008) coupled flow rate to precipitation proportionally to show that dam and terrace patterns could be reproduced using simple rules. Recent modeling (Hammer et al., 2008) that added hydrodynamics, solution chemistry, transport, degassing, and precipitation indicated the importance of another mechanism promoting dam growth: hydrodynamic advection normal to the surface and the compression of vertical concentration gradients as flow supersaturated with respect to calcium carbonate advects over a single dam. However, these assertions have not been tested in experimental or field studies in ambient temperature fluvial systems. Thus, further explanation is needed to address complex fluvial travertine systems in watersheds where repeating travertine patterns are present. In particular, whereas prior field, laboratory, and modeling work document one type of travertine pattern representing travertine bedform morphology such as dams and terraces, documentation of a sequence of disparate but organized fluvial travertine bedforms along the longitudinal profile of a river is lacking.

3. Study area

Jiuzhaigou is situated in the Min Shan Mountains at the eastern margin of the Tibetan Plateau north of the Sichuan basin. The watershed occupies two south-to north-trending valleys, the western Rize valley and the eastern Zechawa valley. Downstream of where they join, the valley is called Shuzheng valley (Fig. 1). Flow from the Jiuzhaigou watershed joins the Baihe River, a tributary to the Yangtze River.

In Jiuzhaigou, the carbonate rocks of Devonian through Triassic age that underlie the watershed are folded and faulted (Zhang and Ge, 2003). Rock units are oriented NW–SE with one set of faults along the same trend as the rock units and a second set of faults approximately perpendicular. Active regional tectonic uplift and tilting (Kirby et al., 2000) create steep slopes conducive to hillslope erosion processes such as debris flows, debris avalanches, rock falls, and slides (Cui et al., 2005). In addition to lithologic and structural variation, fluviokarst processes such as collapse also are likely to contribute to variation in valley gradient and the presence of some lakes.

Along with the natural tectonic, geologic, geomorphic, and hydrologic setting, human activities influence biogeochemical processes and hydraulics within the Jiuzhaigou system. Land use has included farming terraced loess deposits for several millennia in proximity to the nine Tibetan villages within Jiuzhaigou (Harrell et al., 2009; Henck et al., 2009). Logging and associated activities began in 1966 and ceased by 1979 (Zhang and Ge, 2003). Current human activities that influence water quality in the watershed include those associated with tourism of over two million visitors per year (Gaulke et al., 2010). Associated road and trail construction activities may also contribute sediment to the valley bottom. Because of the sensitivity of the travertine landforms to hydrology and water chemistry, additional factors such as climate change and potential acidification from air pollution may be significant threats.

The high basin relief at Jiuzhaigou, ~2070 m, creates climate zones and associated botanical diversity within the forested watershed (Tang, 2006). Precipitation and temperatures are seasonal, with the majority of rainfall occurring between May and October and the highest temperatures occurring between May and September. Watershed hydrology is variable throughout the various climate zones and flow discharges are likely to be seasonal; however, discharge is not gaged in the watershed. Similarly, neither groundwater surface elevations nor flow variability usually characteristic of karst environments is documented. Field reconnaissance suggests that the Rize valley contains a flowing river interspersed with dams and lakes along the majority of its length, in contrast to the Zechawa valley which lacks continuous surface flow. The upper portion of Zechawa valley contains lakes impounded by glacial debris and rock falls, but lacks surface river flow and travertine deposition; the lower portion contains isolated pools in an otherwise dry gravel-bed channel—such as was observed during field reconnaissance in September 2009 and 2010. Thus, our analysis is focused on ~32.7 km of the Rize–Shuzheng system, part of which contains a segment characterized by travertine.

4. Map and image analysis and field methods

We use remotely sensed data to analyze watershed-scale channel gradient, including a 90-m resolution digital elevation model (DEM; 2000 Shuttle Radar Topography Mission (SRTM), http://glcf.umiacs.umd.edu/data/srtm/index.shtml) for the lower two-thirds of the Jiuzhaigou basin extending from the mouth in Shuzheng valley to the headwaters of Rize and Zechawa valleys. In order to avoid apparent artifacts in this data set (such as alignment of contour lines in stripes), analysis of the upper one-third of the watershed was based on available 1:100,000 topographic map with 40 m contour intervals (Sichuan Bureau of Surveying and Mapping). These data were used to construct a ~50-km longitudinal profile extending from the mouth of the basin in Shuzheng valley to the headwaters of Rize valley; gradient is measured between each known contour interval. We focus on the downstream 32.7-km reach between the Primeval Forest and the watershed mouth. Resolution of this topographic data allows for estimation of profile variation in the high relief Jiuzhaigou basin, where the profile is assumed to be an estimate of water-surface elevation, or the energy slope of the river. Analysis of a 2004 QuickBird satellite image (Digital Globe, Inc.) with 2.4-m spatial resolutions four-band multispectral data provided the basis for measurements of channel and valley widths over the entire study area within a Geographic Information System (GIS). Measurement was straightforward except where shadows of adjacent hillslopes obscured the channel or valley margins. Registration between the two data sets with different scales and resolution is a source of uncertainty, thus the two data sets were used independently with the topographic map used to analyze the basin-scale river profile, and the QuickBird image used to analyze width. Future studies may refine longitudinal distance data as higher resolution watershed-scale topographic data become available.

Field data collected during four field campaigns during 2008–2010 included measuring profiles over large travertine dam complexes, smaller travertine bedforms, and measurement of water chemistry. Longitudinal profiles over five large travertine dams were measured using a 5× magnifying hand-held level, a fiber glass tape, and a rod along the edge of the water—because of a restriction against human–water contact in the reserve. Longitudinal profiles measured include: (i) a 500-m profile and cross section transect at Pearl Shoals; (ii) a 560-m profile at Norilang Lakes; (iii) a 1110-m profile that included both Tiger and Shuzheng dams along the left bank from Rhinoceros Lake to Princess Lake (a small lake downstream of Shuzheng Falls); (iv) a 260-m profile along the right bank from Tiger Lake to Princess Lake opposite the profile along the left bank; and (v) a 370-m profile at Bonsai. These data and observations from field reconnaissance provide quantitative local channel gradient data along travertine dams with secondary bedforms defining their surface topography. Topographic variability of the large travertine dams in the cross-channel direction is illustrated by comparing the left-bank to right-bank profiles over Shuzheng Falls and in the cross section of the travertine channel bed measured from the foot bridge across Pearl Shoals. The height of secondary dams shown includes each dam present measured from crest to base along the profile; height of islands is measured from thalweg of intervening channels to topographic high point of adjacent island on the channel bed; height of shoals is estimated from crest to base. The average height of secondary travertine dams includes each dam present along the longitudinal profiles measured at Pearl Shoals and Norilang Lakes. At Pearl Shoals, instantaneous flow velocity was measured from the bank along the profile using a digital Global Water flow probe during September 2008 to show relative differences in between morphologic zones (see data indicated on Fig. 4B).

Water chemistry quantified in the field at 41 sample locations in Rize and Shuzheng valleys during September 2010 included electrical conductivity, EC, total dissolved solids, TDS, and water temperature, T.

Measurements were obtained using an HM COM 100 digital EC and TDS meter (accuracy: ±2%; resolution: 1 μS/ppm) that automatically corrects for temperature. The 2010 sample locations were determined based on the spatial distribution of morphology, e.g. near the head and base of dams and in lakes, and thus were therefore dependent on the spacing of dams and the lakes they impound. Additionally, six sample locations in lakes and wetlands in Zechawa valley measured during September 2009 and 28 sample locations in Rize and Shuzheng valleys were measured during the same field campaign. Although hydrologic conditions were not constant, they were similar over each sampling period. Thus, although trends in spatial variability of the constituents measured are similar, the analysis of the 2009 data is limited to a comparison of water chemistry in Zechawa valley relative to Rize and Shuzheng valleys during the same field campaign. EC and TDS were used as proxies for dissolved calcite to help indicate the spatial extent of the system where travertine is likely to form. The rationale for using EC and TDS as proxies is because of their nature as a measure of the ability of water to conduct an electrical current in proportion to the concentration of positive and negative ions. The majority of TDS load is from four negative ions (bicarbonate, carbonate, chloride, and sulfate) and four positive ions (calcium, magnesium, sodium, and potassium) and TDS is directly proportional to EC. Because groundwater in karst terrain easily dissolves soluble carbonate rocks (Palmer, 1990), sudden elevation of EC and TDS in river water likely represents contributions from springs or discharges of groundwater into the fluvial system.

5. Results

5.1. Water chemistry and the travertine dam segment

Variation in water chemistry measured in September 2010 reveals a spatial association with the presence of travertine dams at Jiuzhaigou. The proxy parameters EC and TDS, used to illustrate favorable conditions for calcite precipitation, vary longitudinally in the channel between the Primeval Forest in Rize valley and the mouth of the Jiuzhaigou watershed in Shuzheng valley. The longitudinal change initiates with a marked increase in EC and TDS coinciding with the upstream position of the travertine segment (Fig. 2). The sudden increase in these water chemistry proxies for dissolved calcite suggests the presence of substantial groundwater discharge to the main river in this location. At the upstream end of the travertine segment near Arrow Bamboo, EC and TDS are elevated by ~30% over values farther upstream. In contrast, at the downstream end of the segment (near Bonsai), EC and TDS are similar to values farther downstream in the reach that lacks travertine (Fig. 2). Values of EC and TDS decrease by ~25% through the travertine segment at a rate of ~0.0034 μS/m (51 μS/14,984 m).

The rate of EC and TDS decrease is not linear within the travertine segment. Instead, the water chemistry proxies decrease in a stepped pattern (Fig. 2), with the highest rates of decrease coinciding with the locations of large travertine dams. Between the base of an upstream travertine dam and the next downstream dam, EC and TDS values increase slightly; whereas the decrease is rapid as water flows over each primary travertine dam (Fig. 2). However, an exception is the Bonsai primary dam where water chemistry does not change appreciably upstream or downstream—thus bracketing the area of influence for ion-rich groundwater contributions to the travertine segment as between about Arrow Bamboo and Bonsai. Values of EC measured in Zechawa valley at six locations in lakes and wetlands throughout the valley in September 2009 are relatively low, averaging within 10% of EC upstream of the travertine reach in Rize valley during the same period—a factor that in combination with the lack of river flow, contributes to the lack of travertine in that tributary system.

5.2. Watershed scale steps and valley width

The longitudinal profile over 32.7 km between the Primeval Forest in Rize valley and the mouth of the basin in Shuzheng valley exhibits steps characterized by higher gradients than intervening lower gradient fluvial and lacustrine reaches (Fig. 3). These steps account for about 50% of the elevation change along the entire basin profile. All of the primary travertine dams at Jiuzhaigou coincide with a watershed-scale step distinguishable in the topographic map and are concentrated within a 16.3-km segment between Arrow Bamboo Falls in Rize valley and Bonsai in Shuzheng valley that coincides with elevated EC and TDS values. At least seven primary travertine dams are present in this reach (Fig. 3). However, one of the dams, Colorful Lake Dam, lacks travertine and appears to be composed of landslide debris. Similarly, dams that impound lakes upstream of the travertine segment such as Grass Lake Dam and Swan Lake Dam appear to be composed of landslide debris and do not contain travertine. One dam present downstream of the travertine segment in Shuzheng valley is a constructed concrete dam.

Measurements made using the high resolution satellite imagery and topographic data revealed the variability in spacing between all of the steps present between Primeval Forest in Rize valley and the mouth of Shuzheng valley. Step spacing ranges from ~0.2 to ~6.5 km with a mean of ~1.9 km. Many of the steps are dams that impound relatively large lakes—where the step is the downstream side of the dam, whereas, the lower gradient reach upstream of the step is the lake. However, not all of the dams are characterized by travertine. Instead they are dams formed by mass movement debris derived from adjacent steep hillslopes. Mean spacing between steps that are travertine dams in lower Rize valley (between Arrow Bamboo dam and Norilang Lakes dam) and Shuzheng valley (between Tiger dam and Bonsai dam) was ~1.30 and ~1.35 km, respectively.

Instead of a progressive downvalley increase in width common to morphometrics in fluvial systems, the Rize–Shuzheng valley includes narrow upstream and downstream segments with an irregularly wider and narrower zone corresponding to the location of the travertine segment. Valley width in the travertine segment is characterized by a marked increase in variability (Fig. 3), with a range from ~5.0 to 340 m and an average of ~148 m. In contrast to the variability of width in the travertine segment, the upstream fluvial reach is relatively narrow and widths are less variable averaging ~21 m. Downstream of the travertine segment, the average width is only 10 m, excluding areas with anthropogenic influence such as the developed park entrance at the valley mouth and the marshy reach immediately upstream of the constructed dam.

5.3. Valley-spanning primary travertine dams and two secondary travertine dam morphologies present atop the downstream side of primary dams

5.3.1. Primary travertine dams

Travertine dam morphologies and sizes are variable in Jiuzhaigou. We term large travertine dams that extend across the entire valley width *primary dams*. Observations from field reconnaissance of the travertine dams present in the watershed within the travertine segment indicate that in the downstream direction, or longitudinally, the majority of the primary travertine dams are asymmetric. For example, the upstream sides of five of the primary travertine dams investigated in this study (Fig. 4A; Pearl Shoals, Norilang Lakes, Tiger, Shuzheng, and Bonsai) are submerged by lakes impounded by the dams; and to the extent visible through the clear water, the submerged travertine appears nearly vertical, albeit rough and irregular. On the upstream side of Bonsai, sediment fill forms a wetland. Field data from the five primary dams investigated quantify the slopes of the downstream sides of the primary travertine dams as ranging from 0.0179 to 0.1143 (Table 1). In contrast to the nearly vertical upstream sides, the downstream sides of these dams extend for distances ranging from about 260 to 536 m, and height from crest to base ranges from ~9 to 44 m (Table 1). Primary dams are longer (in the downstream direction) than wide (in the cross-valley direction) with length-to-width ratios ranging from ~2.6 to 4.7 (Table 1).

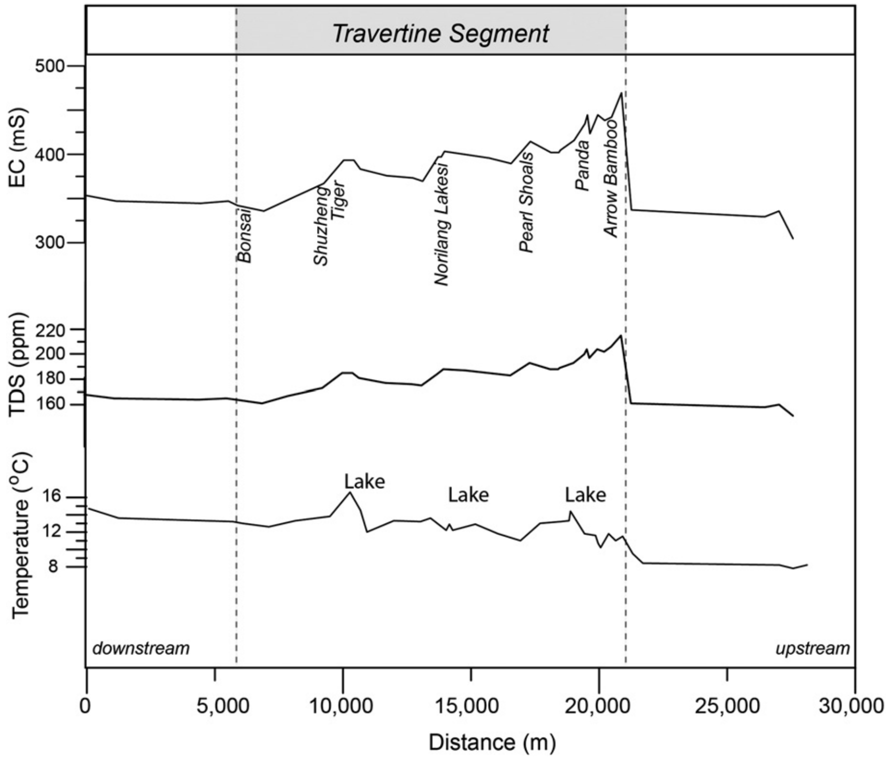

Fig. 2. Longitudinal change in water chemistry initiates with a marked increase in EC and TDS, corresponding spatially to the upstream boundary of the travertine segment with little change at the downstream end of the segment. Within the travertine segment a stepped pattern characterizes the rate of the decline of EC and TDS with the highest rates of decrease corresponding to locations of the primary travertine dams. Temperature generally increases in the downstream direction, with relatively higher values present in lakes upstream of the primary dams.

Debris from hillslope erosion processes is visible in three of the primary travertine dams (Tiger, Shuzheng, and Bonsai) as large boulders present atop the travertine substrate or incorporated into the travertine structures. In contrast, boulders are not visible at two of the primary travertine dams (Pearl Shoals and Norilang Lakes). The shapes of the longitudinal profiles over the downstream sides of Tiger, Shuzheng (left bank profile), and Bonsai primary dams are generally irregular or stepped (Fig. 4A). In contrast, the shape of the longitudinal profile measured over the downstream side of the Pearl Shoals primary is convex (Fig. 4A), and the profile is characterized by variability in slope with lower gradient reaches occurring at the upstream crest of the dam and a transition to a waterfall at the

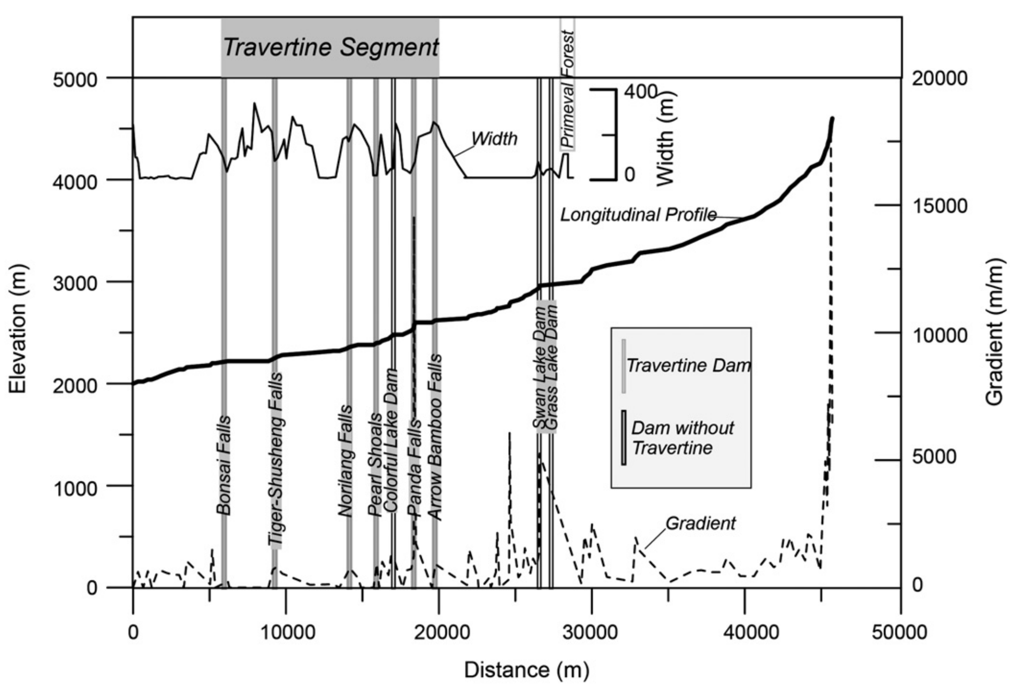

Fig. 3. Steps in the longitudinal profile highlighted by peaks in associated gradient, illustrating associations with travertine and nontravertine dams. Inset shows variation in valley width.

downstream base of the dam. Norilang Lakes has a profile that is quasiconvex, with a steeper reach becoming lower gradient near the base of the dam. We focus next on Pearl Shoals and Norilang Lakes primary travertine dams situated in the lower Rize valley where values of EC and TDS are higher than for those farther downstream (see Fig. 2). Both of these primary travertine dams have heights >30 m, lengths >500 m, and widths of ~190 m, on the same order as valley width (Table 1). Although it is likely that these dams also incorporate contributions from hillslope erosion, their surfaces are dominated by travertine. Notably, they support an array of organized smaller travertine bedforms, including dams, on their downstream sides.

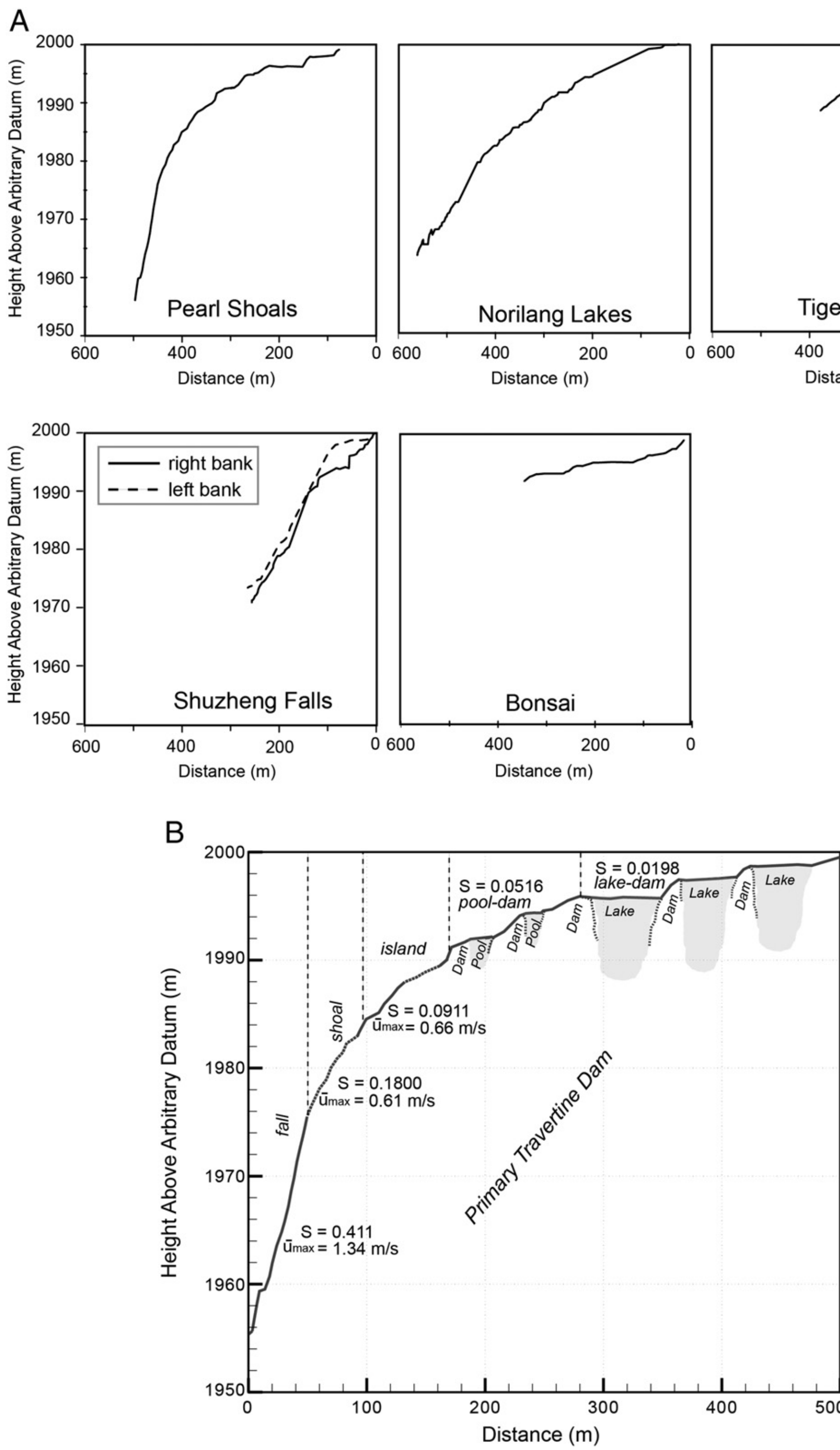

Fig. 4. (A) Longitudinal profiles of the downstream side of five large primary travertine dams showing elevation vs. distance at Pearl Shoals, Norilang Lakes, Tiger Falls, Shuzheng Falls (left and right bank profiles), and Bonsai. Pearl Shoals and Norilang Lakes profiles are quasiconvex, with lower slope present on the upstream portion than on the steeper downstream portions of the profiles. (B) Detailed view of the downstream side of the primary dam profile at Pearl Shoals showing zones of secondary morphology associated with changing slope and average flow velocity (u).

5.3.2. Secondary travertine dams

We term a set of relatively small, repeating travertine bedform patterns, or travertine sequences, present atop the sloping downstream sides of primary travertine dams *secondary* morphology. First, we address two disparate sequences of secondary travertine dam morphologies present at Pearl Shoals and Norilang Lakes. From the lower slope reach near the crest of the primary dam toward the higher slope reach at the downstream base (Fig. 4B), distinctive sequences of secondary morphology include small dams that impound correspondingly small waterbodies. We distinguish two distinct morphologies of secondary dams present atop primary dams as *lake–dams* and relatively smaller *pool–dams*. Table 2 summarizes field data documenting their distinguishing characteristics. Although some similarities exist between the two secondary dam morphologies, differences that distinguish the two types of secondary dams at Jiuzhaigou are significant. Morphologic differences are related to the slope of the portion of the downstream side of the primary dam on which they form (enhanced by longitudinal profile convexity), their size, and their spacing (Tables 1 and 2).

The morphology of both type of secondary dams mimics larger primary travertine dams in some respects: longitudinal profiles appear asymmetric, with nearly vertical and irregular upstream sides. Similarly, in planview, the crests of secondary dams form quasiperpendicular to the longitudinal profile; however, their sides curve such that they connect to the dam upstream. We consider a secondary dam from crest to downstream base together with its upstream waterbody to be a morphologic unit, as the width and height of the dam govern the width and depth of the corresponding upstream waterbody.

Lake–dam sequences form at the upstream end of the array of secondary morphology atop Pearl Shoals and Norilang Lakes primary travertine dams, whereas the relatively smaller pool–dam sequences form downstream of the lake–dam sequences (Table 2; Figs. 4A, B and 5A). As water flows from the downstream portion of relatively deep lakes with depths on the same order as the height of the primary dams they are impounded by, flow shallows and slope increases at the crest of the dam to ~0.010 as it transitions to its sloping downstream side that supports secondary bedforms. Because of the convex nature of the longitudinal profiles of the primary travertine dams, slope in the upstream lake–dam reach is less than further downstream in the pool–dam reach (Table 2; Fig. 4B). The average slope of lake–dam zones present on both primary dams is 0.0167, whereas the slope of pool–dam zones is 0.0711 (Table 2). Fig. 4B illustrates this relationship at Pearl Shoals, where lake–dams form in sequences on slopes of about 0.0198, and pool–dams form farther downstream in sequences in zones with higher slopes of 0.0516. At Norilang Lakes, the upstream succession of lake–dam and pool–dam sequences occurs in zones with similar slopes as those at Pearl Shoals; whereas the downstream set near the base of Norilang Lakes is somewhat steeper (Table 2; 0.052 at Pearl Shoals and 0.066 and 0.103 at the upstream and downstream set at Norilang Lakes, respectively).

Secondary dam widths also provide a metric that distinguishes between relatively wider (in the cross-valley direction) lake–dam and narrower pool–dam sequences. Based on field data from Pearl Shoals and Norilang Lakes, the average of the ratio between secondary lake–dam widths relative to primary dam widths is 0.69; whereas, the ratio is only 0.06 for pool–dam sequences (Tables 1 and 2). The width of the waterbodies impounded by secondary dams is equivalent to the cross-channel width of each dam. Because the number of secondary dams is limited by the dimensions and variability within the primary dam they are formed on, there are a limited number of secondary dams available for analysis in this study. Robust statistical analysis would require numerical simulations to generate an appropriate data set.

Spacing of repeating patterns of secondary dams is another metric that aids in distinguishing the two dam morphologies. Lake–dam sequences have an average spacing from dam crest-to-crest of ~30 m, almost twice the average spacing of ~17 m for pool–dam sequences. Ratios of dam length to waterbody length are governed by the spacing of the repeating travertine patterns. Lengths of both types of secondary dams are shorter than upstream lake lengths. Lake–dam sequences have an average dam-length to waterbody-length ratio of 0.37; whereas in pool–dam sequences, dam length is also less than associated pool lengths—however the average ratio of 0.67 is about twice that for lake–dams.

The ratios of secondary dam length in the direction of the longitudinal profile to cross-channel dam width for both types of secondary dams differ from the relationship in primary dams. Secondary dam length is less than dam width, in contrast to primary dams where the opposite relationship between length and width characterizes the landform (Tables 1 and 2). The average dam-length to dam-width ratio is similar for the two types of secondary dams, with a ratio of 0.31 for lake–dams and 0.32 for pool–dams (Table 2), in contrast to the primary travertine dams where these ratios are g > 1.0, as previously noted (see Table 1).

The fluvial travertine substrate afforded by the secondary dams in Jiuzhaigou supports a vibrant wetland (Fig. 5A and B). Shallow water flowing approximately perpendicular to the crest of each dam appears to be influenced by small hydrophilic trees and shrubs growing on the travertine dams. In particular, pool–dams sometimes incorporate living trees and other organic material into the travertine structure of pool–dams.

5.3.3. Repeating secondary travertine bedforms besides dams influenced by slope

Significantly, distinctive repeating secondary travertine bedforms besides dams are present at Pearl Shoals in succession according to slope (Fig. 4B). These travertine forms include islands and steps, shoals,

Table 1
Physical characteristics of primary travertine dams.

Primary dam	Slope[a]	Dam length (m)	Dam width (m)[b]	Dam height (m)	Upstream impounded lake	Upstream lake length (m)	Hillslope influence (y or n)	Progression of secondary morphology
Pearl Shoals	0.0901	500	193	44.0	Golden Bell Lake	5.1[c]	n	Lake-dam; pool-dam; islands; steps; shoals; falls
Norilang Lakes	0.0700	536[d]	191	36.0	Mirror Lake	0.4	n	Lake-dam; islands; pool-dam; falls
Tiger	0.0246	340	280	9.7	Rhinoceros Lake	0.3	y	Steps; falls
Shuzheng (RB)	0.1139	260	211	29.0	Tiger Lake	1.0	y	Steps; falls
Shuzheng (LB)	0.1177	259	211	26.2				
Bonsai	0.0161	472	100	9.0	Shallow marsh	0.7	y	stEps; falls

[a] Downstream side measured in field measurements from the lip to the base of primary dam.
[b] Measured from aerial imagery except at Pearl Shoals, where width was measured in the field along foot bridge.
[c] Golden Bell Lake upstream of Pearl Shoals dam appears truncated by a landslide on its upstream side.
[d] Norilang primary dam length extends ~20 m beyond measured profile.

Table 2
Physical characteristics of secondary travertine dams.

Secondary morphology	Local reach slope	Height > water surface[a] (m)	Dam length (m)	Width (m)	Lake length (m)
Lake–dam sequences					
Pearl Shoals average (n = 3)	0.0198	1.28	18.7	58.5 to 234	54.4
Norilang average (n = 3)	0.0664; 0.1045	0.35	13.9[b]	47.8 to 191	18.7
Average of all individual forms measured	0.0167	0.91	16.7	53.2	45.5
					Pool length (m)
Pool–dam sequence					
Pearl Shoals average (n = 2)	0.0516	0.24	5.1	na	15.9
Norilang average (n = 18)	0.0912	0.64	3.9	11.4	5.9
Average of all individual forms measured	0.0711	0.58	3.9	11.4	7.4

[a] Height above water surface measured from crest of dam to water surface on downstream side of dam.
[b] Measured length — dam extends ~20 m farther downslope.

and waterfalls. Reaches with travertine islands separated by intervening channels with irregularly spaced travertine steps are present in steeper zones downstream of pool–dam sequences at slopes of 0.0911 (Fig. 4B). Islands have irregular boundaries and are slightly elongated in the direction of flow with length-to-width ratios of ~2.0, average widths of 1.5 m, and average heights of 0.2 m (Fig. 5C and D). The range of widths of intervening channels where flow converges between islands is between 0.1 and 4.5 m, with an average of 1.8 m (Fig. 6). In the same reach, rounded travertine steps are oriented perpendicular to flow, with straight, wavy, or concave upstream patterns—these steps are discontinuous across the channel and form on a travertine surface without apparent plunge pools. At Norilang Lakes, islands are present in steeper zones, but boundaries are diffuse and the structures also appear to form atop secondary dams—as a tertiary bedform. Submerged portions of the islands, steps, and channels at Pearl Shoals are covered with algae; above the water surface, vegetation includes moss, horsetails, grass, shrubs, and small trees.

Travertine shoals form in zones with an average slope of 0.1800 downstream of the island zone on the Pearl Shoals primary dam (Figs. 4B and 5E). The shoals are steep, undulating travertine surfaces that appear to be a succession of small, closely spaced, and rounded steps that produce shallow turbulent flow. The steps are generally elongated in the direction perpendicular to the longitudinal profile but are discontinuous across the channel where the morphology transitions to islands and steps. The height of each step is generally ~0.1 m with a few reaching ~1.0 m in the transition to the downstream waterfall. Boundaries of the shoals also appear diffuse with the steps in the island reach resembling the small steps that comprise the shoals and with some vegetated islands present within the shoals. The shoals include areas with bare travertine and areas where the travertine is substrate for algae, moss, or trees.

Nearly vertical waterfalls often characterize either a portion or the majority of the downstream edge of primary travertine dams (Fig. 4). The slope of the falls at Pearl Shoals is ~0.4110. In contrast, the flow path along the measured profile at the edge of water at Norilang Lakes bypassed the waterfall present on the opposite bank. Waterfalls have irregular shapes along their top edges (Fig. 5F), likely because downstream extension of the falls occurs through travertine deposition that creates overhangs that are subject to mass failure—creating wavy patterns caused by resulting protrusions or indentations along the top edge of the fall. Field observation suggests that eroded blocks of travertine and/or other debris at the base of the falls reach about two-thirds of total fall height.

5.3.4. Other travertine bedforms and crusts

Other travertine bedforms are recognized at primary dams that appear to be dominated by boulders derived from landslides. Secondary morphology includes boulder steps incorporated into or on the surface of travertine substrate (Fig. 5G; e.g., Tiger–Shuzheng Falls and Bonsai). Boulder steps atop the downstream side of travertine dams influenced by landslide debris are present at a wider range of slopes (ranging from 0.0216 to 0.1315) than the steps that occur together with islands at Pearl Shoals. Boulders are visible as part of the structure in Shuzheng Falls, suggesting that the falls originated at a valley step created as a result of hillslope mass movement processes, with subsequent travertine deposition later modifying the dam structure. Rocky steps atop Tiger and Shuzheng primary dams are spaced ~13.7 m apart with heights of ~0.9 m on average. The presence of boulders arranged in steps suggests that these bedforms are mobile until stabilized by travertine deposition. In contrast, large boulders with median diameters estimated as 1.0 to 2.0 m atop the travertine of the primary dam at Bonsai do not appear mobile.

Travertine crusts on channel and lake beds or on protrusions into the flow are present intermittently throughout the travertine segment (Fig. 5H). Crusts occur on abiotic sediment, such as cobbles and boulders that act as roughness elements, and on organic material such as roots, logs, algae, and moss. Travertine is also apparent on lake bottoms. Crystals may detach and be transported downstream in the river's flow—some may be trapped in lakes where they settle and form travertine lake-bed crusts, and some may be transported out of the Jiuzhaigou system or dissolved in water with lower dissolved calcite concentrations. Calcite crystals entrained in flow would be likely to deposit in wide and deep lakes impounded upstream of dams where flow velocity is low—a possible contributing factor to travertine crusts observed on lake bottoms.

5.4. Secondary morphology slope vs. height power law

Secondary travertine bedforms are present atop Pearl Shoals' and Norilang Lakes' primary travertine dams in zones with slopes ranging between ~0.010 and 0.300 (Fig. 4A and B). This secondary morphology includes bedforms with decreasing height that correspond to increasing slope related to position along profiles on the downstream side of the primary dams. Using the data available, we propose a method to quantify the relation between the secondary travertine bedform height (y) and slope of the profile in the zone of the secondary morphology (x) on the downstream side of primary dams as a power law where $y = 0.0053x^{-1.68}$ (Fig. 7). Assuming that the variables are independent, the power law has a negative exponent indicating that secondary travertine bedform height decreases with increasing slope, consistent with observations that small travertine dams and terraces (Ekmekci et al., 1995; Dreybrodt and Gabrovsek, 2009) and larger travertine dams (Pentecost, 2010) become smaller with increasing slope. We consider the power function relationship preliminary; however, we include it because of its relevance toward understanding scale-invariant morphologies. Uncertainty in this relation based on the field data collected at Jiuzhaigou could be constrained through future detailed field investigations in other travertine fluvial systems, in experimental investigations, or in numerical simulations that quantify the effect of slope variation on travertine bedform height.

6. Discussion

6.1. What factors determine the spatial distribution of large travertine dams?

Results of our investigation at Jiuzhaigou address the question of why primary travertine dams form where they do. We present a conceptual model whereby the spatial locations of primary dams are governed by water chemistry, basin-scale changes in channel gradient

Fig. 5. Photographs showing examples of secondary morphology: (A) lake–dam sequences; (B) pool–dam sequences; (C) multiple islands; (D) islands and steps; (E) shoals; (F) waterfall; (G) rock steps; and (H) examples of other travertine forms (such as fluvial crusts on bryophyte, roots, logs in channel incorporated into dam). Distinctive sequences of secondary travertine morphology are present atop the downstream side of primary travertine dams at Pearl Shoals and Norilang Lakes. Arrows indicate flow direction.

at steps, and variation in valley width. First we address the significance of water chemistry as a factor in governing where travertine precipitation is possible. All of the primary travertine dams at Jiuzhaigou are present within a segment of Rize and Shuzheng valleys with elevated levels of EC and TDS. Thus, initiation of the travertine segment at Jiuzhaigou coincides spatially with the marked change in water chemistry where EC and TDS increase by ~25% (see Fig. 2). Using EC and TDS as proxies for dissolved calcite in river water illustrates that after the dissolved calcite concentration of the river water increases above an apparent threshold, C_i, travertine precipitation is possible; however, variation in water chemistry alone does not explain the spatial distribution of primary travertine dams in the Jiuzhaigou fluvial system. Thus, we address geomorphic parameters such as slope that varies at steps in the longitudinal profile as the second component of the conceptual model.

All of the primary travertine dams at Jiuzhaigou coincide with steps in the longitudinal profile. Steps in a longitudinal profile may result from numerous factors that indicate regional or local controls on gradient such as lithologic changes (Moglen and Bras, 1995), the presence of faults (Seeber and Gornitz, 1983; Kirby et al., 2003), landslide dams (Korup et al., 2006), or transitions between zones where different processes operated in the past such as the glacial to fluvial transition at the start of the Holocene (Hobley et al., 2010). Further,

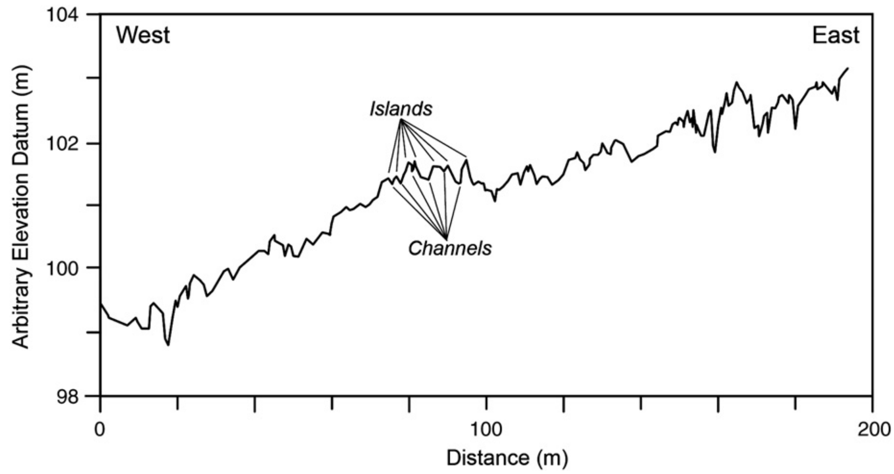

Fig. 6. Cross section measured along footbridge across Pearl Shoals showing geometry of Islands (topographic high points and intervening channels (topographic low points). Note the strong asymmetry in average channel bed slope from east to west.

fluviokarst groundwater–surface water interactions at Jiuzhaigou may alter longitudinal profile development by causing sudden changes in surface water discharge, or by creating conditions for characteristic collapse structures on the valley bottom. At Jiuzhaigou, many of these factors may interact to create the steps that disrupt an ideally convex-shaped profile where slope and particle size decrease as discharge increases with distance downstream (Mackin, 1948).

Steps in the longitudinal profile are significant at Jiuzhaigou because they influence the spatial location of primary travertine dam formation. Pentecost (2010) noted that large dams appear to form at slope breaks or in association with landslide debris but that little else is known about their genesis. Mechanisms of primary travertine formation at steps are likely related to the abrupt local increase in channel slope that, in turn, increases flow velocity. Increased velocity is associated with travertine deposition (Hammer et al., 2007) either because flow acceleration lowers water pressure, thereby accelerating release of dissolved CO_2 gas (Chen et al., 2004), or alternatively because higher flow velocity causes thinning of a diffusion-limiting boundary layer where CO_2 conversion and calcite precipitation take place (Buhman and Dreybrodt, 1985a,b; Liu et al., 1995; Liu and Dreybrodt, 1997).

Once travertine deposition is initiated at a step in the longitudinal profile, continued travertine deposition increases the step height, with the depth of the lake impounded upstream approximating the height of the travertine dam. As formation of a travertine dam increases step height, local gradient steepens and flow velocity increases downstream, thus creating a positive feedback such that travertine precipitation preferentially takes place in that location. The convex form of the profile of some of the primary travertine dams investigated at Jiuzhaigou (e.g., Pearl Shoals; see Fig. 4B) is such that the steepest slopes and highest velocity flows are at the downstream end of the structure. This observation supports modeling results (Hammer et al., 2007) suggesting that as dam crests grow in height, they prograde in the downstream direction and thus are dynamic features. In contrast, some of the primary travertine dams have quasilinear or stepped profiles (e.g., Tiger Falls; see Fig. 4A). On a smooth slope, travertine precipitation could tend toward equivalence along the profile. However, in a steep forested environment such as Jiuzhaigou, irregularities in a smooth profile could be caused by the influence of landslide debris, large woody debris, or live trees that modify hydrodynamics governing local travertine precipitation rates. Reaches without travertine deposition also occur within the travertine segment at Jiuzhaigou; thus we infer that the absence of steep steps may be significant in limiting travertine deposition even though water chemistry may be favorable.

We address valley width as the third parameter governing the spatial location of primary dams at Jiuzhaigou. In Jiuzhaigou, valley width does not progressively increase downstream, likely reflecting differential erosion rates in the folded and fractured carbonate terrain and from variation common to fluviokarst terrain. The travertine segment in Jiuzhaigou coincides with a zone with large variability in valley width that is on average 7 to 15 times wider than upstream and downstream reaches without travertine, respectively. Width variation is an important consideration in investigating the spatial distribution of travertine precipitation because of its potential influence in causing changes in flow hydrodynamics that Chen et al. (2004) documented as associated with travertine precipitation. In particular, valley width could influence velocity associated with flow convergence and divergence. Although flow divergence in the lateral dimension in wider reaches may lower flow velocity, the shallowing of flow may cause flow convergence in the vertical dimension. In either case, shallowing of flow lowers fluid pressure. It follows that travertine is more likely to be deposited in shallow wide reaches with lower bed fluid pressure than in deeper, narrow reaches with higher fluid pressure, a mechanism that may provide a rationale to overcome effects of widening in decreasing flow velocity. Deeper flow has higher fluid pressure that may limit the CO_2 degassing required for travertine formation—this factor may compound water chemistry as a factor in precluding travertine deposition downstream of the travertine reach. Wider channel reaches in Jiuzhaigou have greater channel-bed surface area than narrow channels, providing greater potential crystal nucleation and travertine deposition over the larger contact area. Furthermore, molecular diffusion is enhanced in the shallow and wide reaches where a greater surface area to water volume ratio creates a greater potential for CO_2 degassing as well as delivery of ions from solution to growing travertine bedforms. Thus, primary travertine dam initiation is more likely to occur within the wider reaches of the travertine segment than in narrower upstream or downstream reaches.

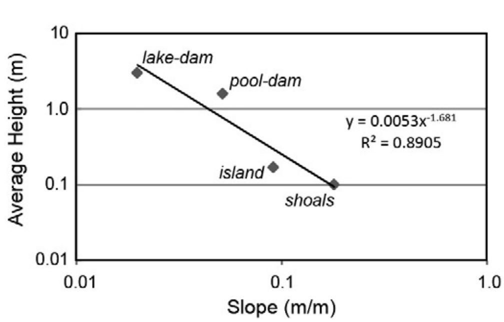

Fig. 7. A power function quantifies the decrease in secondary travertine form height with increasing slope.

After initiation of a primary travertine dam, as flow from a lake impounded upstream approaches the crest of the dam, flow depth decreases, and velocity accelerates over the constriction at the sill. This increase in velocity relative to the slow flow in the lake promotes travertine deposition at the crest of the dam. Flow is routed through notches or lower areas on the dam crest, and travertine is preferentially deposited in these areas, raising elevation and realigning flow toward a lower portion of the crest. Thus, dam height is self-limiting, and the dam crest is maintained at a relatively level elevation across the width of the structure. Moreover, the dam crest may extend laterally until constrained by valley walls—which provides a primary constraint on dam width.

6.2. What factors control variability of secondary travertine morphology?

Field data collected in Jiuzhaigou illustrate an array of secondary travertine bedforms that form atop the downstream side of primary travertine dams, a distinct travertine morphology in Jiuzhaigou. These data inform a new classification of travertine bedforms, including dam morphologies and other macroforms that differ from previous work including sequences of lake–dams, pool–dams, islands and steps, and shoals. In contrast to travertine bedforms where deposition predominates, waterfalls form a boundary where mechanical erosion and travertine depositional processes interact and determine the longitudinal extent, or length, of the primary dam.

We propose a conceptual model supported by the field data collected at Jiuzhaigou that addresses the influence of slope on secondary travertine morphology. First, we propose upper and lower slope thresholds that characterize the physical conditions required for precipitation of travertine bedforms. A lower slope threshold of ~0.010 and an upper slope threshold of ~0.300 are present at the upstream crest and downstream base of primary travertine dams, respectively. At Pearl Shoals, secondary dams transition to islands and shoals at slopes >~0.070, whereas, dams are absent in a steep zone at Norilang Lakes where slope exceeds ~0.150. Thus, the slope thresholds correspond to observed discontinuities in secondary travertine morphology. Slopes steeper than the upper threshold occur as flow descends waterfalls.

To explain why morphologic discontinuities appear in association with changes in slope, we propose a rationale for the upper and lower slope thresholds based on the influence of slope on flow velocity. First, with respect to the upper slope threshold, increases in flow velocity are associated with increases in travertine precipitation rates (Chen et al., 2004). Moreover, velocity changes influence advection of calcium carbonate in near-bed flow, a critical factor in travertine deposition (Hammer, 2009). Thus, the upper slope threshold may correspond to the point where the ratio of flow rate relative to travertine precipitation rate exceeds a critical value. This critical value, in turn, corresponds to a critical point where hydrodynamic advection of calcium carbonate cannot be sustained normal to the surface, a condition for travertine precipitation noted by Hammer et al., 2008—thus limiting travertine precipitation. With respect to the lower slope threshold, slope is too low and flow depth too deep in waterbodies such as pools or lakes upstream of dams for conditions that promote degassing and for travertine precipitation to occur. In contrast, on the downstream side of the dams, such conditions prevail.

To explain morphologic discontinuities between the upper and lower slope threshold (e.g., associated with transitions from lake–dams to pool–dams, or pool–dams to islands, or islands to shoals), we hypothesize that secondary travertine bedforms act as roughness elements that cause resistance to water flowing over the downstream side of primary travertine dams. On average, spacing of dams decreases by about 57% from lake–dam to pool–dam sequences. The transition from lake–dam to smaller and more closely spaced pool–dam sequences (Table 1) suggests that although pool–dam height is less than lake–dam height, pool–dams maximize roughness and energy losses because their sequences are more closely spaced, analogous to maximization of relative roughness in alluvial channels, e.g., Robinson and Albertson (1952). Thus, field data from Jiuzhaigou support a hypothesis whereby the height and spacing offered by the secondary travertine dams influences the slope and velocity of upstream and downstream flow. Secondary morphology forming on the downstream face of primary dams increases surface roughness and thus flow resistance. Flow resistance is relatively high in the shallow flow on the downstream face of the dam where the height of secondary travertine forms (h_T) or boulder steps (d_s) relative to flow depth (d) is large. We infer that the resistance factors h_T/d or d_s/d cause turbulence that aerates flow, causes bubbles, and forms spray—all increasing the air–water interface area, that, in turn, lowers the fluid pressure, enhances CO_2 degassing, and promotes travertine precipitation as described in Chen et al. (2004). It follows that the development of secondary morphology at Jiuzhaigou is strongly linked to local hydrodynamics.

In the cross-channel direction, hydrodynamic variation caused by convergence of flow in narrow, deep zones and divergence of flow in wider, shallow zones at the scale of the secondary morphology likely influences travertine deposition by creating variability in fluid pressure. For example, in reaches with travertine islands and intervening channels, the channels have relatively greater flow depths and correspondingly higher fluid pressures that may limit deposition, in contrast to the turbulent flow along the margins of the islands and shallower flow over their surfaces that promotes precipitation. Lower fluid pressure also results from the relatively high velocity flows on the downstream face of primary travertine dams and, in turn, enhances travertine precipitation. Asymmetry of bed elevation in the cross channel direction likely responds to variation in travertine deposition rates due to variable flow velocity caused by vegetation establishment, hillslope debris, or due to positive feedback related to travertine deposition itself.

Slope is a main influence on river hydrodynamics. Slope influences and is influenced by secondary travertine morphology that forms as a result of hydrodynamics that favor travertine deposition. Further, once formed, travertine bedforms modifies flow dynamics in a positive feedback that promotes their own growth (Goldenfeld et al., 2006; Jettestuen et al., 2006; Chan and Goldenfeld, 2007; Hammer et al., 2007). At Jiuzhaigou, we find not only does local channel slope seem to control travertine bedform morphology but that these secondary morphologies also locally modify the slope of the longitudinal profile, creating a local feedback mechanism. Furthermore, we suggest that the spatial scale of the downstream side of primary travertine dams that contains an array of disparate forms is the relevant scale to investigate secondary travertine morphology.

Secondary morphology documented in field data from Jiuzhaigou appears scale invariant with respect to the relation illustrated in the slope vs. height power law (see Fig. 7). As slope steepens, bedform height decreases, consistent with the observation that travertine rimstone dam and terrace structures (e.g., Dreybrodt and Gabrovsek, 2009) become smaller with increasing slope. The height of secondary travertine bedforms controls the energy gradient of the upstream flow and exerts control over local travertine precipitation. In this way, topographic irregularities in the travertine surface created by secondary morphology are self-sustaining in that they promote travertine precipitation that enhances secondary morphology and simultaneously increases the height of the primary travertine dam. In Jiuzhaigou, secondary lake–dam and pool–dam sequences appear quasi-self-similar in morphology to primary travertine dams and the lakes they impound despite differences in slope and spacing, consistent with Chan and Goldenfeld's (2007) suggestion that travertine forms are scale-invariant and that travertine precipitation rates are characterized by nonlinearity because the travertine surface changes as travertine precipitates. Scaling relations describing dam length to cross channel dam width of ~0.30 represent all of the dam bedforms at Jiuzhaigou—including primary dams, lake–dams and pool–dams—suggesting that in one-dimensional aspect scale is invariant in travertine dams, despite the diversity inherent in the forested system in Jiuzhaigou. Differences in other scaling aspects may be attributed to the role of large woody debris and hydrophilic trees that are incorporated into the travertine dams in the forested watershed or to travertine dams associated with landslide debris that influences dam location, dam height, and lake lengths. For example, hydrophilic trees growing in the travertine substrate and obstructions (such as travertine-encrusted logs incorporated into travertine bedforms) compound hydrodynamic heterogeneity and variability in morphology of the secondary travertine forms and, when incorporated into the bedform, enhance the growth rate.

Formation of travertine structures in ambient temperature fluvial systems in forested watersheds such as Jiuzhaigou is influenced by sediment transport and by large woody debris. Travertine precipitation may be precluded in fluvial reaches with mobile sediment where travertine precipitated on clasts is abraded during transport or where high rates of aggradation of sediment derived from erosive hillslopes may inhibit crystal nucleation or bury incipient travertine structures. Alternatively, travertine precipitation may be enhanced in fluvial reaches with local availability of sites for nucleation of calcite crystals created by diversity within the fluvial system.

6.3. Implications for conservation of fluvial travertine landforms

The steep terrain at Jiuzhaigou, situated at the margin of the Tibetan Plateau, is sensitive to human activities (Tang, 2006). Since 2002, over two million visitors tour Jiuzhaigou annually (Tang, 2006). Travertine landforms are vulnerable to environmental change and are degraded when travertine precipitation ceases as a result of changes in water chemistry, sediment load, trampling, or changes in hydrology (Pentecost et al., 2000). Recent work has also shown that increased levels of phosphates related to anthropogenic inputs inhibit travertine deposition (Zhang et al., 2012). Thus, parameters including climate, flow discharge and hydraulics, slope, vegetation, tectonics, and human activity are suggested as being important in fluvial travertine formation. Results of this study add to the scientific basis for developing sustainable management strategies to preserve fluvial travertine landforms at Jiuzhaigou. Specifically, understanding factors that govern travertine development and the potential for human activities to alter these processes is one critical element in developing biodiversity conservation strategies. First, because travertine precipitation is a water-dependent process, sustaining the natural variability of river flow magnitude, duration, frequency, timing, and rates of change of river flow is imperative. Because of the strong linkage between surface water and groundwater in karst environments that underlie the travertine landforms, sustaining groundwater levels is imperative to achieving the goal. Second, because travertine formation is a chemical process, water chemistry plays a critical role. Addition of contaminants such as heavy metals, nutrients, and sediment that alter microbial function or wetland vegetation may modify the spatial distribution and rates of travertine formation as well as its solubility and dissolution. Further, our results suggest that travertine morphology is sensitive to geomorphic parameters such as slope and width. Thus conservation strategies that protect geomorphic characteristics of the fluvial system will aid in the protection of the diversity of travertine landforms and the ecosystems that depend on them.

7. Conclusions

This remote sensing and field study investigated the geomorphology of a contemporary ambient temperature fluvial travertine system in Jiuzhaigou, China, in order to address two fundamental questions. First, what factors determine the spatial distribution of large travertine dams? Second, what factors influence the secondary morphology of the array of distinct bedforms present atop these primary dams? At Jiuzhaigou, three factors are paramount in determining the spatial locations of primary, or large, valley-spanning travertine dams. These irregularly spaced large travertine dams are formed at watershed-scale steps in the longitudinal profile in a segment with high variability in valley width, where a water chemistry proxy value for dissolved calcite is above an apparent threshold. Smaller secondary travertine morphology atop the downstream side of convex-shaped primary dams includes an array of forms associated with local slope. Slope, which must provide favorable hydrodynamics and fluid pressures that in turn influence CO_2 release and travertine precipitation, appears to govern the development of discrete patterns of repeating travertine bedforms. From relatively low to higher slopes, these forms include lake–dam sequences, pool–dam sequences, travertine islands and step sequences, shoals, and waterfalls. Secondary morphology on the downstream side of primary dams where landslide debris creates a watershed-scale step in the longitudinal profile includes boulder steps and waterfalls partially encrusted with travertine. Unique to forested fluvial travertine systems, field observations suggest that large woody debris derived from forested hillslopes is incorporated within travertine forms and likely is a significant factor in the initiation and growth rates of travertine structures.

Results of this study are fundamental toward an understanding of travertine river systems at two scales: the fluvial system scale, where primary travertine dams are influenced by and influence longitudinal profile development, and the local scale of individual large travertine dams, where smaller secondary travertine morphology is organized as an array of bedforms associated with local slope. The data presented provide baseline data that may be used in future investigations to understand spatial variability and dynamics of travertine morphology, growth rates, and evolution. These results provide a new basis for future experimental and modeling studies to comprehensively understand the dynamics of fluvial travertine landscapes.

Acknowledgments

We thank Dean Winston Ko, Gretchen Kalonji, Louise Kellogg, and Peter Schiffman, University of California, Davis, and the Jiuzhaigou Administrative Bureau, China, for their support of this research collaboration. Helpful discussion and field assistance was provided by Li Bing, Yu Bo, Li Jing, Paul Haverkamp, Zhang Song, and Hu Xinxin. We are grateful for the field equipment and insight provided by Dawn Sumner and the suggestions from anonymous reviewers. This project received support from the China 111 project (B08037) and the University of California Office of the President International Seed Grant program.

References

Andrews, J.E., 2006. Paleoclimatic records from stable isotopes in riverine tufas: synthesis and review. Earth-Science Reviews 75, 85–104.
Andrews, J.E., Riding, R., Dennis, P.F., 1993. Stable isotopic compositions of recent freshwater cyanobacterial carbonates for the British Isles; local and regional environmental controls. Sedimentology 40, 303–314.
Buhman, D., Dreybrodt, W., 1985a. The kinetics of calcite dissolution and precipitation in geologically relevant situation of karst areas: 1. open system. Chemical Geology 48, 189–211.
Buhman, D., Dreybrodt, W., 1985b. The kinetics of calcite dissolution and precipitation in geologically relevant situation of karst areas: 2. closed system. Chemical Geology 53, 109–124.
Carthew, K.D., Taylor, M.P., Drysdale, M.P., 2006. An environmental model of fluvial tufas in monsoonal tropics, Barkly karst, northern Australia. Geomorphology 73, 78–100.
Chan, P.Y., Goldenfeld, N., 2007. Steady states and linear stability analysis of precipitation pattern formation at geothermal hot springs. Physical Review E 76, 046104.
Chen, J., Zhang, D.D., Wang, S., Xiao, T., Huang, R., 2004. Factors controlling tufa deposition in natural waters at waterfall sites. Sedimentary Geology 166, 353–366.
Cui, P., Liu, S., Tang, B., Chen, X., Zhang, X., 2005. Debris Flow Study and Prevention in National Parks. Science Press, Beijing, China, pp. 90–96.
Dreybrodt, W., Gabrovsek, F., 2009. Small-scale terraces and isolated rimstone pools on stalagmites in caves exhibit striking similarity to large-scale terrace landscapes at hot springs. Acta Carsologica 38 (1), 19–26.
Ekmekci, M., Gunay, G., Sinsek, S., 1995. Morphology of rimstone pools at Pamukkale, western Turkey. Cave and Karst Science 22, 103–106.
Ford, T.D., Pedley, H.M., 1992. Tufa deposits of the world. Journal of Speleological Society, Japan 17, 46–63.
Ford, T.D., Pedley, H.M., 1996. A review of tufa and travertine deposits of the world. Earth-Science Reviews 41, 117–175.
Foulke, B.W., 2011. Hot-Spring Systems Geobiology: Abiotic and Biotic Influences on Travertine Formation at Mammoth Hot Springs. Sedimentology Decade Review, Yellowstone National Park, USA.

Fuller, B.M., Sklar, L.S., Xompson, Z.G., Adams, K.J., Marks, J.C., Wilcox, A.C., 2011. Ecogeomorphic feedbacks in regrowth of travertine step-pool morphology after dam decommissioning, Fossil Creek, Arizona. Geomorphology 126, 314–332.
Gaulke, L.S., Weiyang, X., Scanlon, A., Henck, A., Hinkley, T., 2010. Evaluation criteria for implementation of a sustainable sanitation and wastewater treatment system at Jiuzhaigou National Park, Sichuan Province, China. Environmental Management 45, 93–104.
Goldenfeld, N., Chan, P.Y., Veysey, J., 2006. Dynamics of precipitation pattern formation at geothermal hot springs. Journal of Physical Research Letters 96, 254501.
Golubic, S., 1973. The relationship between blue-green algae and carbonate deposits. In: Carr, N.G., Whitton, B.A. (Eds.), The Biology of Blue-green Algae. Blackwell, Oxford, UK, pp. 434–472.
Hammer, O., Dysthe, D.K., Lelu, B., Lund, H., Meakin, P., Jamtveit, B., 2008. Calcite precipitation instability under laminar, open-channel flow. Geochemica et Cosmochimica Acta 72, 5009–5021.
Hammer, O., 2009. Pattern formation by local amplification and lateral inhibition: examples from biology and geology. The European Physical Journal of Special Topics 178, 5–12.
Hammer, O., Dysthe, D.K., Jamtveit, B., 2007. The dynamics of travertine dams. Earth and Planetary Science Letters 256, 258–263.
Harrell, S., Hinkley, T.M., Hagmann, R.K., Taylor, J.W., Yang, Q., et al., 2009. A Partnership for Biodiversity in a Chinese National Park. University of Washington, East Asia Center(3 pp.).
Henck, A., Taylor, J., Lu, H., Li, Y., Yang, Q., Grub, B., Breslo, S.J., Robbins, A., Elliot, A., Hinckley, T., Combs, J., Urgenson, L., Widder, S., Hu, X., Ma, Z., Yuan, Y., Jian, D., Liao, X., Tang, Y., 2009. Anthropogenic hillslope terraces and swidden agriculture in Jiuzhaigou National Park, northern Sichuan, China. Quaternary Research 73, 201–207.
Herman, J.S., Lorah, M.M., 1987. CO_2 outgassing and calcite precipitation in Falling Spring Creek, Virginia, USA. Chemical Geology 62, 251–262.
Herman, J.S., Lorah, M.M., 1988. Calcite precipitation rates in the field: measurement and prediction for a travertine-depositing stream. Geochimica et Cosmochimica Acta 52, 2347–2355.
Hobley, D.E.J., Sinclair, H.D., Cowie, P.A., 2010. Processes, rates, and timescales of fluvial response in an ancient postglacial landscape of the northwest Indian Himalaya. Geological Society of America Bulletin 122, 1569–1584.
Jettestuen, E., Jamtveit, B., Podladchikov, Y.Y., deVilliers, S., Amundsen, H.E.F., Meakin, P., 2006. Growth and characterization of complex mineral surfaces. Earth and Planetary Science Letters 249, 108–118.
Kirby, E., Whipple, K.X., Burchfiel, B.C., Tang, W., Berger, G., Sun, Z., Chen, Z., 2000. Neotectonics of the Min Shan, China: implications for mechanisms driving Quaternary deformation along the eastern margin of the Tibetan Plateau. GSA Bulletin 112 (3), 375–393.
Kirby, E., Whipple, K.X., Tang, W., Chen, Z., 2003. Distribution of active rock uplift along the eastern margin of the Tibetan Plateau: inferences from bedrock channel longitudinal profiles. Journal of Geophysical Research 108 (B4), 2217.
Korup, O., Strom, A.L., Weidinger, J.T., 2006. Fluvial response to large rock-slope failures: examples for the Himalayas, the Tien Shan, and the Southern Alps in New Zealand. Geomorphology 78, 3–21.
Liu, Z., Dreybrodt, W., 1997. Dissolution kinetics of calcium carbonate minerals in H_2O–CO_2 solutions in turbulent flow. Geochimica et Cosmochimica Acta 61, 2876–2889.
Liu, Z., Scensson, U., Dreybrodt, W., Daoxian, Y., Buhman, D., 1995. Hydrodynamic control of inorganic calcite precipitation in Huanglong Ravine, China: field measurements and theoretical prediction of deposition rates. Geochimica et Cosmochimica Acta 59 (15), 3087–3097.
Lu, G., Zheng, C., Donahoe, R.J., Lyons, W.B., 2000. Controlling processes in a $CaCO_3$ precipitating stream in Huanglong Natural Scenic District, Sichuan, China. Journal of Hydrology 230, 34–54.
Mackin, J.H., 1948. Concept of the graded river. GSA Bulletin 59, 463–512.
Merz-Preiss, M., Riding, R., 1999. Cyanobacterial tufa calcification in two freshwater streams: ambient environment, chemical thresholds and biological processes. Sedimentary Geology 125, 103–124.
Moeyersons, J., Nyssen, J., Poesen, J., Deckers, J., Haile, M., 2005. Age and backfill/overfill stratigraphy of two tufa dams, Tigray Highlands, Ethiopia: evidence for Late Pleistocene and Holocene wet conditions. Palaeo 230, 165–181.
Moglen, G.E., Bras, R.L., 1995. The importance of spatially heterogeneous erosivity and the cumulative area distribution within a basin evolution model. Geomorphology 12 (3), 173–185.
Palmer, A.N., 1990. Groundwater processes in karst terranes. In: Higgins, C.G., Coates, D.R. (Eds.), Groundwater Geomorphology: the Role of Subsurface Water in Earth — Surface Processes and Landforms: Boulder, Colorado, Geological Society of America Special Paper, 252, pp. 177–209.
Pedley, H.M., Rogerson, M., 2010. Tufas and speleothems: unraveling the microbial and physical controls. The Geological Society, London, Special Publication, 336 (367 pp.).
Pedley, M., Martin, J.A.G., Delgado, S.O., 2003. Sedimentology of quaternary perched springline and paludal tufas: criteria for recognition, with examples from Guadalajara Province, Spain. Sedimentology 50 (1), 23–44.
Pena, J.L., Sancho, C., Lozano, M.V., 2000. Climatic and tectonic significance of late Pleistocene and Holocene Tufa Deposits in the Miljares River canyon, eastern Iberian Range, northeast Spain. Earth Surface Processes and Landforms 25 (13), 1403–1417.
Pentecost, A., 2005. Travertine. Springer, Berlin(445 pp.).
Pentecost, A., 2010. Travertine. Springer, Berlin(445 pp.).
Pentecost, A., Viles, H., 1994. A review and assessment of travertine classification. Geographie Physique et Quaternaire 48, 305–314.
Pentecost, A., Zhang, Z., 2000. The travertine flora of Jiuzhaigou and Munigou, China and its relationship with calcium carbonate deposition. Cave Karst Science 27, 71–78.
Pentecost, A., Zhang, Z., 2001. A review of Chinese Travertine. Cave Karst Science 28, 15–28.
Pentecost, A., Peterken, G.F., Viles, H.C., 2000. The travertine dams of Slade Brook, Gloucestershire: their formation and conservation. Geology Today 22–25.
Riding, R., 2000. Microbial carbonates: the geological record of calcified bacterial–algal mats and biofilms. Sedimentology 47 (Suppl. 1), 179–214 (36).
Robinson, A.R., Albertson, M.L., 1952. Artificial roughness standard for open channels. Transactions of the American Geophysical Union 33, 881–888.
Seeber, L., Gornitz, V., 1983. River profiles along the Himalayan arc as indicators of active tectonics. Tectonophysics 92 (4), 335–337.
Tang, Y., 2006. Introduction of Sichuan University and Jiuzhaigou National Park and a proposal for a UCD and SCU research workshop on ecological and environmental sustainability of Jiuzhaigou Park. Drafted by Tang Ya, Executive Director Jiuzhaigou International Laboratory for Ecology, Environment and Sustainability, Sichuan University. (5 pp.).
Veysey, J., Goldenfeld, N., 2008. Watching rocks grow. Nature Physics 4, 310–313.
Viles, H., Goudie, A., 1990. Tufas, travertines, and allied carbonate deposits. Progress in Physical Geography 14, 19–41.
Viles, H., Pentecost, A., 1999. Geomorphological controls on tufa deposition at Nash Brook, South Wales, United Kingdom. Cave and Karst Science 26, 61–68.
Wright, J.S., 2000. Tufa accumulations in ephemeral streams: observations from the Kimberley, north-west Australia. Australian Geographer 31 (3), 333–347.
Zhang, X., Ge, N., 2003. Jiuzhaigou — the Heritage for All Mankind(121 pp.).
Zhang, D.D., Zhang, Y., Zhu, A., Cheng, X., 2001. Physical mechanisms of river waterfall tufa (travertine) formation. Journal of Sedimentary Research 71 (1), 205–216.
Zhang, J., Wang, H., Liu, Z., An, D., Dreybrodt, W., 2012. Spatial–temporal variations of travertine deposition rates and their controlling factors in Huanglong Ravine, China — a world heritage site. Applied Geochemistry 27, 2011–2222.